Derivative-Free Design Optimization of Sonnet-Simulated Structures Using Shape-Preserving Response Prediction and Space Mapping

Slawomir Koziel

Engineering Optimization & Modeling Center, School of Science and Engineering,
Reykjavik University, 101 Reykjavik, Iceland
koziel@ru.is

Abstract: A two-level derivative-free algorithm for design optimization of structures simulated using Sonnet ***em*** is introduced. The presented technique exploits a coarse-discretization model of the structure of interest that is optimized on a coarse grid using pattern search. Space mapping optimization is subsequently performed with the underlying surrogate model created using limited amount of coarse-discretization Sonnet model data and a recently introduced shape-preserving response prediction methodology. Our technique is demonstrated through the design of two microstrip filters.

Keywords: Computer-Aided Design (CAD), Electromagnetic Simulation, Derivative-Free Optimization, Microwave Design, Shape-Preserving Response Prediction

1. Introduction

EM-simulation-based design closure becomes increasingly important in contemporary microwave engineering. This is partially due to a growing demand for accuracy but also because design-ready theoretical models are not easily available for many structures such as UWB antennas or substrate-integrated circuits. On the other hand, simulation-driven optimization may be impractical because of its high computational cost, particularly in the case of traditional (e.g., gradient-based) algorithms that require large number of EM simulations.

Low-cost simulation-driven design can be performed using surrogate model: a computationally cheap representation of the structure under consideration. The surrogate model is iteratively updated and re-optimized in order to yield a satisfactory design of the original structure [1]. It is of primary importance for the computational efficiency of this process that the surrogate is physically based [2] so that it can give a reliable prediction of the original structure's behavior under the modification of its designable parameters.

The most successful techniques in microwave engineering exploiting physically-based surrogates are (SM) [2]-[5] and various forms of tuning [6]-[8] and tuning SM [9,10]. The tuning approaches are particularly suited to be used with Sonnet ***em*** [11] because of its co-calibrated ports technology [8]. It should be noted though that implementation of both SM and tuning is not always straightforward: substantial modification of the optimized structure may be required (tuning), or additional mapping and more or less complicated interaction between auxiliary models is necessary (SM). Also, space mapping performance heavily depends on the surrogate model selection [12]. A simple yet efficient design optimization methodology to be used with Sonnet ***em*** was introduced in [13], which was based on sequential optimization of coarsely-discretized Sonnet models of increasing mesh density and the design refinement using an auxiliary second-order polynomial model.

In this paper, an alternative technique is proposed that exploits space mapping working with a surrogate model constructed using the coarse-discretization Sonnet-simulation data and a modified version of the shape-preserving response prediction (SPRP) [14] technique. Our method does not require any circuit-equivalent coarse model or any modification of the structure being optimized. The surrogate model created using SPRP is more accurate than the polynomial approximation used in [13], which allows us to conduct the design process using a limited number of evaluations of a single coarse-discretization Sonnet model. Our technique is demonstrated through the design of two microstrip filters.

2. Design Optimization Using Shape-Preserving Response Prediction and Space Mapping

A. Design Optimization Problem

The design optimization problem is formulated as follows:

$$\boldsymbol{x}_f^* \in \arg\min_{\boldsymbol{x}} U(\boldsymbol{R}_f(\boldsymbol{x})), \tag{1}$$

where $\boldsymbol{R}_f(\boldsymbol{x}) \in R^m$ is a response vector of a structure of interest, e.g., $|S_{21}|$ at m frequencies; $\boldsymbol{x} \in R^n$ is a design variable vector; U is a scalar merit function, e.g., a minimax function with upper/lower specifications; $\boldsymbol{x}_f^*$ is the optimal design to be determined. Here, $\boldsymbol{R}_f$ is evaluated using Sonnet ***em*** with a $g_{h.f} \times g_{v.f}$ grid.

B. Coarse-Discretization Model and Initial Optimization Stage

The optimization technique introduced here exploits a coarse-discretization model $\boldsymbol{R}_{cd}$, also evaluated using Sonnet ***em***. The model $\boldsymbol{R}_{cd}$ exploits a grid $g_{h.c} \times g_{v.c}$ so that $g_{h.c} > g_{h.f}$ and $g_{v.c} > g_{v.f}$.

The model $\boldsymbol{R}_{cd}$ is optimized on the grid $g_{h.c} \times g_{v.c}$ using a pattern search algorithm [13] in order to find a design $\boldsymbol{x}^{(0)}$ that will be used as a starting point for the next optimization stage. Obviously, the resolution of this initial optimization stage is limited by the coarseness of the grid $g_{h.c} \times g_{v.c}$, however, for the same reason, the computational cost of finding $\boldsymbol{x}^{(0)}$ is low and typically corresponds to a few evaluations of the fine model $\boldsymbol{R}_f$.

C. Surrogate Model Construction Using Shape-Preserving Response Prediction

Having optimized the coarse-discretization model $\boldsymbol{R}_{cd}$ we also have its evaluations at $\boldsymbol{x}^{(0)}$ and at all perturbed designs around it, $\boldsymbol{x}_k^{(0)} = [x_1^{(0)} \ldots x_k^{(0)} + \mathrm{sign}(k)\cdot d_k \ldots x_n^{(0)}]^T$, i.e., $\boldsymbol{R}^{(k)} = \boldsymbol{R}_{cd}(\boldsymbol{x}_k^{(0)})$, $k = -n, -n+1, \ldots, -1, 1, \ldots, n-1, n$. Here, $d_k = g_{h.c}$ or $g_{v.c}$ (depending on the orientation of $x_k^{(0)}$ with respect to $x^{(0)}$). This data is used to build the surrogate model for the subsequent space mapping optimization process. The surrogate is constructed following the shape-preserving response prediction (SPRP) technique [14] which is modified here because no underlying coarse model is available in our case. We shall use the notation $\boldsymbol{R}_{cd}(\boldsymbol{x}) = [R_{cd}(\boldsymbol{x},\omega_1) \ldots R_{cd}(\boldsymbol{x},\omega_m)]^T$, where ω_j, $j = 1, \ldots, m$, is the frequency sweep.

Figure 1 shows the response of the coarse-discretization model at $\boldsymbol{x}^{(0)}$, $\boldsymbol{R}_{cd}(\boldsymbol{x}^{(0)})$, as well as the response of $\boldsymbol{R}_{cd}$ at $\boldsymbol{x}_k^{(0)}$ for a certain value of k. The plots are $|S_{21}|$ responses of the microstrip bandpass filter considered in Section 3.*A*. A set of characteristic points is distinguished on each of the plots, here, corresponding to $|S_{21}| = -5$ dB, -20 dB, as well as local $|S_{21}|$ maxima and minimum within the pass band. A discussion on how to select characteristic points for a specific design case can be found in [14]. We use the notation $\boldsymbol{p}_0^j = [\omega_0^j \ r_0^j]^T$ and $\boldsymbol{p}_k^j = [\omega_k^j \ r_k^j]^T$, $j = 1, \ldots, K$, to denote characteristic points of $\boldsymbol{R}_{cd}(\boldsymbol{x}^{(0)})$ and $\boldsymbol{R}_{cd}(\boldsymbol{x}_k^{(0)})$, respectively. Here, ω and r denote the frequency and magnitude components of the respective point. The short line segments shown in Fig. 1 are so-called translation vectors defined as $\boldsymbol{t}_k^j = [\omega_{t.k}^j \ r_{t.k}^j]^T$, $j = 1, \ldots, K$, where $\omega_{t.k}^j = \omega_k^j - \omega_0^j$ and $r_{t.k}^j = r_k^j - r_0^j$. The translation vectors indicate the change of the characteristic points of the $\boldsymbol{R}_{cd}$ response while moving from $\boldsymbol{x}^{(0)}$ to $\boldsymbol{x}_k^{(0)}$.

In order to employ SPRP to predict the response of $\boldsymbol{R}_{cd}$ at any $\boldsymbol{x}$ we have to find the translation vectors $\boldsymbol{t}^j = [\omega_t^j \ r_t^j]^T$, $j = 1, \ldots, K$, corresponding to the change of design from $\boldsymbol{x}^{(0)}$ to $\boldsymbol{x}$. For any given design $\boldsymbol{x}$, we find a subset X_S of the base set $\{\boldsymbol{x}_k^{(0)}\}$ that defines a rectangular area (hypercube) containing $\boldsymbol{x}$. The surrogate model is set up using all points from X_S. Figure 2 illustrates this for $n = 2$. Without loss of generality, we can assume that $X_S = \{\boldsymbol{x}^{(0)}, \boldsymbol{x}_1^{(0)}, \ldots, \boldsymbol{x}_n^{(0)}\}$. We define:

$$\boldsymbol{t}^j = \beta_1 \boldsymbol{t}_1^j + \beta_2 \boldsymbol{t}_2^j + \ldots + \beta_n \boldsymbol{t}_n^j, \tag{2}$$

where $\beta_1, \beta_2, \ldots, \beta_n$, determines a unique representation of $\boldsymbol{x} - \boldsymbol{x}^{(0)}$ using vectors $\boldsymbol{v}_i = \boldsymbol{x}_k^{(0)} - \boldsymbol{x}^{(0)}$, $i = 1, \ldots, n$. Coefficients β_i can be explicitly found as

$$\begin{bmatrix} \beta_1 \\ \beta_2 \\ \\ \beta_n \end{bmatrix} = \left[\boldsymbol{v}_1 \ \boldsymbol{v}_2 \ldots \boldsymbol{v}_n \right]^{-1} \cdot (\boldsymbol{x} - \boldsymbol{x}^{(0)}) \cdot \tag{3}$$

Having the translation vectors $\boldsymbol{t}^j$ we can define the SPRP surrogate model $\bar{\boldsymbol{R}}_s$ of $\boldsymbol{R}_{cd}$:

$$\bar{\boldsymbol{R}}_s(\boldsymbol{x}) = [\bar{R}_s(\boldsymbol{x}, \omega_1) \ \ldots \ \bar{R}_s(\boldsymbol{x}, \omega_m)]^T , \tag{4}$$

where the model $\bar{R}_s$ is defined at frequencies $\omega_0^j + \omega_t^j$, $j = 0, 1, \ldots, K, K+1$, as follows (here, $\omega_0^0 = \omega_1$, $\omega_0^{K+1} = \omega_m$, and $\omega_t^0 = \omega_t^{K+1} = 0$):

$$\bar{R}_s(\boldsymbol{x}, \omega_0^j + \omega_t^j) = \bar{R}_{cd}(\boldsymbol{x}^{(0)}, \omega_0^j) + r_t^j , \tag{5}$$

for $j = 1, \ldots, m$. For other frequencies, the model $\bar{R}_s$ is obtained through linear interpolation:

$$\bar{R}_s(\boldsymbol{x}, \omega) = \bar{R}_{cd}(\boldsymbol{x}^{(0)}, (1-\alpha)\omega_0^j + \alpha\omega_0^{j+1}) + [(1-\alpha) r_t^j + \alpha r_t^{j+1}], \tag{6}$$

where $\omega_0^j + \omega_t^j \leq \omega \leq \omega_0^{j+1} + \omega_t^{j+1}$ and $\alpha = [\omega - (\omega_0^j + \omega_t^j)]/[(\omega_0^{j+1} + \omega_t^{j+1}) - (\omega_0^j + \omega_t^j)]$. $\bar{R}_{cd}(\boldsymbol{x}^{(0)}, \omega)$ is an interpolation of $\{R_{cd}(\boldsymbol{x}^{(0)}, \omega_1), \ldots, R_{cd}(\boldsymbol{x}^{(0)}, \omega_m)\}$ onto the frequency interval $[\omega_1, \omega_m]$. This interpolation is necessary because the original frequency sweep is a discrete set.

Note that the SPRP model (2)-(6) is well defined only if there is one-to-one correspondence between the characteristic points for all responses $\boldsymbol{R}_{cd}(\boldsymbol{x}^{(0)})$ and $\boldsymbol{R}_{cd}(\boldsymbol{x}_k^{(0)})$. Such a correspondence can be enforced even if the number of distinctive features (e.g., local maxima and minima) is different for the responses. One solution is to introduce additional points that are equally spaced in frequency and located in between of other, well defined points [15].

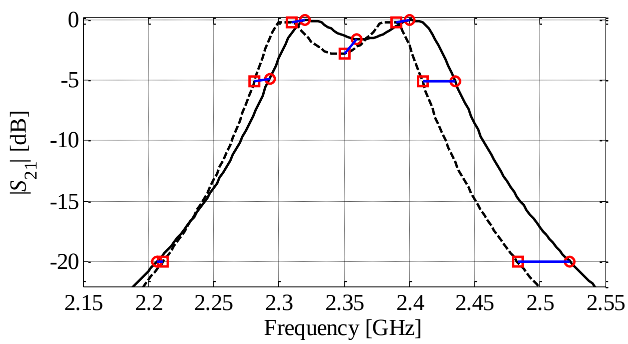

Fig. 1. Example response of the coarse-discretization model $\boldsymbol{R}_{cd}$ at $\boldsymbol{x}^{(0)}$, $\boldsymbol{R}_{cd}(\boldsymbol{x}^{(0)})$, (solid line) and at $\boldsymbol{x}_k^{(0)}$, $\boldsymbol{R}_{cd}(\boldsymbol{x}_k^{(0)})$, (dashed line). Circles and squares indicate the characteristic points of $\boldsymbol{R}_{cd}(\boldsymbol{x}^{(0)})$ and $\boldsymbol{R}_{cd}(\boldsymbol{x}_k^{(0)})$, respectively. Short line segments denote the translation vectors that show the change of the characteristic points of the $\boldsymbol{R}_{cd}$ response while moving from $\boldsymbol{x}^{(0)}$ to $\boldsymbol{x}_k^{(0)}$.

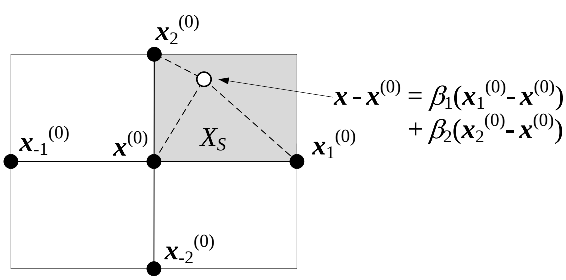

Fig. 2. Utilization of $\boldsymbol{R}_{cd}(\boldsymbol{x}^{(0)})$ and $\boldsymbol{R}_{cd}(\boldsymbol{x}_k^{(0)})$ to create the SPRP surrogate model ($n = 2$). Designs $\boldsymbol{x}^{(0)}$ and $\boldsymbol{x}_k^{(0)}$, $k = -2, -1, 1, 2$, are denoted using black circles. A shaded area denotes a hypercube defined by a subset X_S of points being the closest to an example evaluation design $\boldsymbol{x}$, which is represented as linear combination of vectors $\boldsymbol{x}_k^{(0)} - \boldsymbol{x}^{(0)}$. The translation vectors $\boldsymbol{t}^j$ used to define the surrogate model (2)-(6) at $\boldsymbol{x}$ are calculated using coefficients of this linear combination and the translation vectors of $\boldsymbol{R}_{cd}(\boldsymbol{x}_k^{(0)}) - \boldsymbol{R}_{cd}(\boldsymbol{x}^{(0)})$. Here, we have $\boldsymbol{t}^j = \beta_1 \boldsymbol{t}_1^j + \beta_2 \boldsymbol{t}_2^j$.

D. Space Mapping Optimization Algorithm

The SPRP surrogate model is used to optimize the fine model using the standard space mapping algorithm of the form [2]:

$$\boldsymbol{x}^{(i+1)} = \arg\min_{\boldsymbol{x}} U\left(\boldsymbol{R}_s^{(i)}(\boldsymbol{x})\right), \tag{7}$$

where $\boldsymbol{x}^{(i)}$, i = 0, 1, … is a series of approximate solutions to (1) with $\boldsymbol{x}^{(0)}$ being the approximate optimum of the coarse-discretization model $\boldsymbol{R}_{cd}$ (cf. Section 3.*C*).

In this work, the SPRP model $\bar{\boldsymbol{R}}_s$ is corrected using input and frequency SM [3] so that the SM surrogate model $\boldsymbol{R}_s^{(i)}$ is defined as:

$$\boldsymbol{R}_s^{(i)}(\boldsymbol{x}) = \boldsymbol{R}_s(\boldsymbol{x},[\boldsymbol{c}^{(i)}, f_1^{(i)}, f_2^{(i)}]) = [\bar{R}_s(\boldsymbol{x}+\boldsymbol{c}^{(i)}, f_1^{(i)} + f_2^{(i)}\omega_1) \ \ldots \ \bar{R}_s(\boldsymbol{x}+\boldsymbol{c}^{(i)}, f_1^{(i)} + f_2^{(i)}\omega_m)]^T, \tag{8}$$

where

$$[\boldsymbol{c}^{(i)}, f_1^{(i)}, f_2^{(i)}] = \arg\min_{[\boldsymbol{c}, f_1, f_2]} \sum_{k=0}^{i} \| \boldsymbol{R}_f(\boldsymbol{x}^{(k)}) - \boldsymbol{R}_s(\boldsymbol{x}^{(k)},[\boldsymbol{c}, f_1, f_2]) \| . \tag{9}$$

Using these simple SM transformations is normally sufficient: the SPRP model is relatively accurate by itself as it is built from the coarsely-discretized Sonnet model $\boldsymbol{R}_{cd}$.

3. Illustration Examples

A. Compact Stacked Slotted Resonators Microstrip Bandpass Filter [16]

Consider the stacked slotted resonators bandpass filter [16] shown in Fig. 3. The design parameters are $\boldsymbol{x} = [L_1\ L_2\ W_1\ S_1\ S_2\ d]^T$ mm. The filter is simulated in Sonnet ***em*** [11] using a grid of 0.05 mm × 0.05 mm (model $\boldsymbol{R}_f$). The design specifications are $|S_{21}| \geq -3$ dB for 2.35 GHz $\leq \omega \leq$ 2.45 GHz, and $|S_{21}| \leq -20$ dB for 1.9 GHz $\leq \omega \leq$ 2.3GHz and 2.6 GHz $\leq \omega \leq$ 2.9 GHz. The initial design is $\boldsymbol{x}^{init}$ = [7.2 10.4 0.5 1 2 1.2]^T mm.

The coarse-discretization model $\boldsymbol{R}_{cd}$ uses a grid of 0.4 mm × 0.5 mm. The evaluation times for $\boldsymbol{R}_{cd}$ and $\boldsymbol{R}_f$ are 25 s and 16 min, respectively. Figure 4(a) shows the responses of $\boldsymbol{R}_{cd}$ at $\boldsymbol{x}^{init}$ and at $\boldsymbol{x}^{(0)}$ = [6 9.6 1 1 2 2]^T mm, its optimal design found using a pattern search. Figure 4(b) shows the responses of the fine model at $\boldsymbol{x}^{(0)}$ and at $\boldsymbol{x}^{(2)}$ = [6.15 9.2 1.05 0.9 2.15 2.25]^T mm (minimax specification error –2 dB), the optimal design obtained in two iterations of the SM algorithm using the SPRP surrogate model. The total optimization cost (Table 1) corresponds to only 4 evaluations of the fine model.

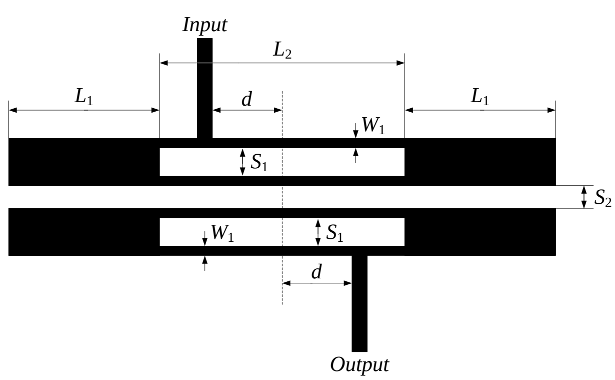

Fig. 3. Stacked slotted resonators filter: geometry [16].

Table 1. Optimization cost of the stacked slotted resonators bandpass filter.

Algorithm Component	Number of Model Evaluations	Computational Cost	
		Absolute [min]	Relative to $\boldsymbol{R}_f$
Optimization of the coarse-discretization model $\boldsymbol{R}_{c.1}$	27	11	0.7
Evaluation of the original (fine-discretization) model $\boldsymbol{R}_f$	3	48	3.0
Total optimization time	N/A	59	3.7

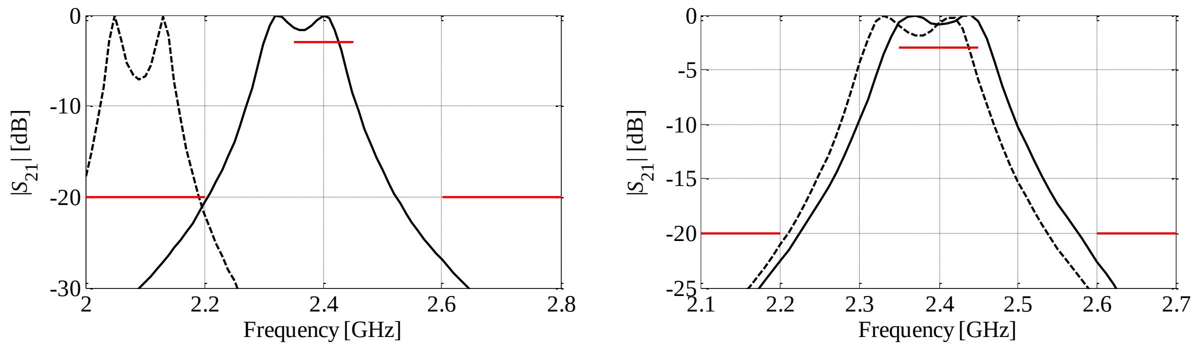

(a) (b)

Fig. 4. Stacked slotted resonators filter: (a) responses of the coarse-discretization model $\boldsymbol{R}_{cd}$ at the initial design $\boldsymbol{x}^{init}$ (dashed line) and at its optimized design, $\boldsymbol{x}^{(0)}$, (solid line); (b) responses of the fine model $\boldsymbol{R}_f$ at $\boldsymbol{x}^{(0)}$ (dashed line) and at the final design $\boldsymbol{x}^{(2)}$ (solid line).

B. Third-Order Chebyshev Bandpass Filter [17]

Consider the third-order Chebyshev bandpass filter [17] shown in Fig. 5. The design variables are $\boldsymbol{x} = [L_1\ L_2\ S_1\ S_2\ W_1\ W_2]^T$ mm. The fine model $\boldsymbol{R}_f$ is simulated in Sonnet ***em*** [11] using a grid of 0.1 mm × 0.02 mm (evaluation time 15 min). The design specifications are $|S_{21}| \geq -1$ dB for 1.8 GHz ≤ ω ≤ 2.2 GHz, and $|S_{21}| \leq -20$ dB for 1.0 GHz ≤ ω ≤ 1.55GHz and 2.45 GHz ≤ ω ≤ 3.0 GHz. The initial design is $\boldsymbol{x}^{init} = [15\ 15\ 0.4\ 0.4\ 0.4\ 0.4]^T$ mm.

The coarse-discretization model $\boldsymbol{R}_{cd}$ uses a grid of 1.0 mm × 0.1 mm (evaluation time 55 s). Figure 6(a) shows the responses of $\boldsymbol{R}_{cd}$ at $\boldsymbol{x}^{init}$ and at $\boldsymbol{x}^{(0)} = [15\ 15\ 0.4\ 0.7\ 0.2\ 0.4]^T$ mm, its optimal design found using a pattern search. Figure 6(b) shows the responses of the fine model at $\boldsymbol{x}^{(0)}$ and at $\boldsymbol{x}^{(2)} = [15.3\ 14.7\ 0.42\ 0.72\ 0.16\ 0.42]^T$ mm (minimax specification error –0.32 dB), the optimal design obtained in two iterations of the SM algorithm using the SPRP surrogate model. The optimization cost (Table 2) corresponds to 6 evaluations of the fine model.

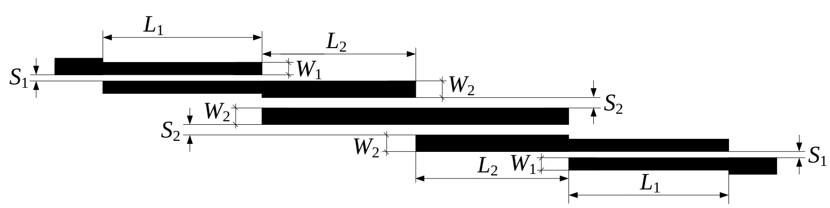

Fig. 5. Third-order Chebyshev bandpass filter: geometry [17].

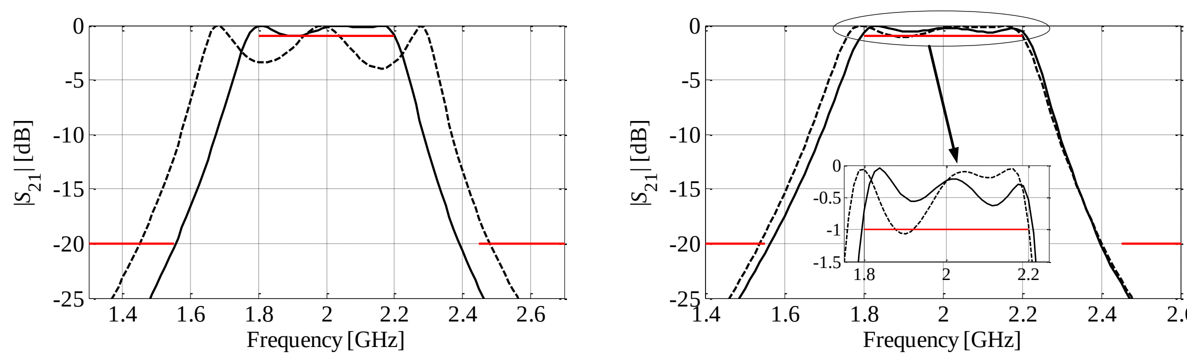

(a) (b)

Fig. 6. Third-order Chebyshev bandpass filter: (a) responses of the coarse-discretization model $\boldsymbol{R}_{cd}$ at the initial design $\boldsymbol{x}^{init}$ (dashed line) and at its optimized design, $\boldsymbol{x}^{(0)}$, (solid line); (b) responses of the fine model $\boldsymbol{R}_f$ at $\boldsymbol{x}^{(0)}$ (dashed line) and at the final design $\boldsymbol{x}^{(2)}$ (solid line).

Table 2. Optimization cost of the third-order Chebyshev bandpass filter.

Algorithm Component	Number of Model Evaluations	Computational Cost	
		Absolute [min]	Relative to $\boldsymbol{R}_f$
Optimization of the coarse-discretization model $\boldsymbol{R}_{c.1}$	48	44	2.9
Evaluation of the original (fine-discretization) model $\boldsymbol{R}_f$	3	45	3.0
Total optimization time	N/A	89	5.9

4. Conclusion

Simple and reliable derivative-free algorithm for microwave design optimization with Sonnet is proposed that utilizes a coarse-discretization Sonnet model of the structure under consideration. This coarse-discretization model is used to obtain the initial approximation of the design as well as to create a fast and accurate surrogate model for subsequent space mapping optimization of the original structure. Our technique is demonstrated through the design of two microstrip filters.

Acknowledgement

The author thanks Sonnet Software, Inc., Syracuse, NY, for ***em***™. This work was supported in part by the Reykjavik University Development Fund under Grant T10006.

References

[1] A.I.J. Forrester and A.J. Keane, "Recent advances in surrogate-based optimization," *Prog. in Aerospace Sciences*, vol. 45, no. 1-3, pp. 50-79, Jan.-April, 2009.

[2] S. Koziel, Q.S. Cheng, and J.W. Bandler, "Space mapping," *IEEE Microwave Magazine*, vol. 9, no. 6, pp. 105-122, Dec. 2008.

[3] J.W. Bandler, Q.S. Cheng, S.A. Dakroury, A.S. Mohamed, M.H. Bakr, K. Madsen, and J. Søndergaard, "Space mapping: the state of the art," *IEEE Trans. Microwave Theory Tech.*, vol. 52, no. 1, pp. 337-361, Jan. 2004.

[4] S. Amari, C. LeDrew, and W. Menzel, "Space-mapping optimization of planar coupled-resonator microwave filters," *IEEE Trans. Microwave Theory Tech.*, vol. 54, no. 5, pp. 2153-2159, May 2006.

[5] G. Crevecoeur, L. Dupre, and R. Van de Walle, "Space mapping optimization of the magnetic circuit of electrical machines including local material degradation," *IEEE Trans. Magn.*, vol. 43, no 6, pp. 2609-2611, June 2007.

[6] D. Swanson and G. Macchiarella, "Microwave filter design by synthesis and optimization," *IEEE Microwave Magazine*, vol. 8, no. 2, pp. 55-69, Apr. 2007.

[7] J.C. Rautio, "EM-component-based design of planar circuits," *IEEE Microwave Magazine*, vol. 8, no. 4, pp. 79-90, Aug. 2007.

[8] J.C. Rautio, "Perfectly calibrated internal ports in EM analysis of planar circuits," *IEEE MTT-S Int. Microwave Symp. Dig.*, Atlanta, GA, pp. 1373-1376, June 2008.

[9] S. Koziel, J. Meng, J.W. Bandler, M.H. Bakr, and Q.S. Cheng, "Accelerated microwave design optimization with tuning space mapping," *IEEE Trans. Microwave Theory and Tech.*, vol. 57, no. 2, pp. 383-394, 2009.

[10] Q.S. Cheng, J.W. Bandler, and S. Koziel, "Space mapping design framework exploiting tuning elements," *IEEE Trans. Microwave Theory and Tech.*, vol. 58, no. 1, pp. 136-144, 2010.

[11] ***em***™ Version 12.54, Sonnet Software, Inc., 100 Elwood Davis Road, North Syracuse, NY 13212, USA, 2009.

[12] S. Koziel, J.W. Bandler, and K. Madsen, "Quality assessment of coarse models and surrogates for space mapping optimization," *Optimization and Engineering*, vol. 9, no. 4, pp. 375-391, 2008.

[13] S. Koziel, "Multi-fidelity multi-grid design optimization of planar microwave structures with Sonnet," *Int. Review of Progress in Applied Comp. Electromagnetics*, April 26-29, Tampere, Finland, 2010, pp. 719-724.

[14] S. Koziel, "Efficient optimization of microwave circuits using shape-preserving response prediction," *IEEE MTT-S Int. Microwave Symp. Dig*, Boston, MA, pp. 1569-1572, 2009.

[15] S. Koziel, "Rapid optimization of microwave structures with FEKO using shape-preserving response prediction," *Int. Review of Progress in Applied Comp. Electromagnetics*, April 26-29, Tampere, Finland, 2010, pp. 35-40.

[16] C.L. Huang, Y.B. Chen, and C.F. Tasi, "New compact microstrip stacked slotted resonators bandpass filter with transmission zeros using high-permittivity ceramics substrate," *Microwave Opt. Tech. Lett.*, vol. 50, no. 5, pp. 1377-1379, May 2008.

[17] J. T. Kuo, S. P. Chen, and M. Jiang, "Parallel-coupled microstrip filters with over-coupled end stages for suppression of spurious responses," *IEEE Microwave and Wireless Comp. Lett.*, vol. 13, no. 10, pp. 440-442, Oct. 2003.